Autonomous Robotics: Demonstrating the Embodiment of Dynamic Field Theory

Evelina Dineva and John P. Spencer
Department of Psychology, University of Iowa, and
Iowa Center for Developmental and Learning Sciences,
Iowa City, Iowa, U.S.A.

Christian Faubel, Yulia Sandamirskaya,
and Gregor Schöner
Institut für Neuroinformatik, Ruhr-Universität Bochum,
Bochum, Germany

***Abstract*—To which extent can cognition be studied separately of the sensorimotor systems that support goal-directed action? In an ongoing debate within developmental science, the embodiment and situatedness stance postulates that understanding cognition requires understanding its close link to the sensory and motor surfaces, its dependence on structured environments and on behavioral context. Although the neuronally based Dynamic Field Theory (DFT) has been proposed as a theoretical framework for the embodiment and situatedness stance, most DFT models have not themselves been embodied nor situated in real environments. This paper shows, that DFT provides the concepts required to embody cognition by implementing the DFT account for perseverative sensorimotor decision making on an autonomous robot. The implementation uses very simple motor control and a very elementary vision system. Reproducing the *A*-not-*B* experimental paradigm with the robot, the robotic model quantitatively reproduces data from human infants. When the robot is enabled to freely move in a structured environment using the same DFT model, the mechanism of habit formation, which leads to perseveration, is shown to stabilize sensorimotor decisions. The robot model of older infants, in contrast, uses self-stabilized neuronal representations to achieve the same goal with the added advantage of flexiblity as task demands vary.**

I. Introduction

Dynamical Field Theory (DFT) is a neurally based theoretical framework for understanding embodied cognition. DFT models are used in a wide range of fields to formulate process models of behavior. For instance, saccadic decision making [1], [2] or manual movement preparation [3] can be explained by the evolution of activation governed by inputs and internal neuronal interactions. Changing the characteristics of neuronal interactions can capture developmental changes in memory-guided infant reaching [4] and later changes in spatial cognition via the spatial precision hypothesis [5]. More recently, DFT has been extended to account for the complex looking patterns of infant visual habituation [6] and even higher cognitive processes like visual working memory and change detection [7].

A. How embodied is DFT?

Typically the models that use DFT concepts are not really situated in the real word, nor do they have a body. It is a central claim of DFT, however, that it satisfies the constraints imposed by situatedness and embodiment, a claim that we investigate here.

The embodied cognition approach proposes that behavior arises when the coupled dynamics of the mind, body, and environment is in a stable state [8]. DFT models are grounded in the world as they use continuous metric dimensions—most prominently space. Space is used to bind features of other dimensions [7]. This allows inputs to be presented with the same metrics, schedule, and intensities as in the experiments. Inputs are integrated in the dynamic field and stimulate neuronal interactions that can form stable attractor states in the field [1], [3]. This stability is a necessary for the cognitive guidance of behavior.

Grounding in metric dimensions and stabilization by neural interactions are prerequisites for embodiment. Therefore, it should be straight forward to implement a DFT model on a robot and let it act upon its world. We do this, using the most elementary from of cognition: a sensorimotor selection of decisions.

B. A-not-B: Infant Sensorimotor Selection Task

Infants' capacity to select sensorimotor goals is ideal for a robot implementation as it is a minimal cognitive task in which infants perform well, as they are not puzzled by the absence of an imperative stimulus. All one needs to consider is how the task situation attracts responses. Decision selection is studied in the A-not-B task with infants [9]–[11]. In this task an infants is confronted with two identical target locations. First, the infant is habituated to reach to one location in a series of A trials: A cue is presented at the A location and after a delay, the infant is allowed to reach, which is typically correct to A. Next, this habit is brought into conflict with the cue: On the B trials, the cue is presented at the alternative B location. After a delay, 7 to 11 month old infants typically make the A-not-B error—reaching to A on a B trial. This is also called perserveration. How much infants perseverate depends on their age and the delay length [10]. In particular, infants over 12 months are correct.

We implement the DFT account for the A-not-B task [4], [12] on an autonomous robot. We demonstrate how decision selection and initiation are continuously linked to the sensory surface. No special properties of the perceptual and motor systems are required to quantitatively match of the infant data (age-delay dependence of perseveration).

The robotic implementation is also a proof of sufficiency of the sensory stream to inform decision making, and that there are no hidden problems in interfaces that do part of the cognitive work. For instance, an alternative Parallel Distributed Processing (PDP) account of the A-not-B task [13] uses a connectionist network where the input units stand for objects (lids or toys). In an autonomous system, it is not straight forward to realize "units" that do higher cognition like object detection. Note that this points to a real distinction between the DFT and connectionist accounts for the A-not-B task.

Another important difference between the DFT and PDP approaches is the focus of DFT on the importance of stability. The robotic demonstration highlights that stabilizing decisions is a crucial—but often overlooked—work that the nervous system does to support behavior.

C. Beyond A-not-B

We also test the robot outside the narrow experimental paradigm of A-not-B. It is placed in an arena where it can move around autonomously, attracted by targets and repelled from obstacles. The questions we ask are: What does it buy the robot to build a habit (motor memory)? What does it buy the robot to have working memory? The free behavior demonstrates that both habit formation (causing perserveration) in young infants and self-sustained activation via neural interactions in older infants are forms of behavioral stabilization.

II. Methods

For this experiment we use a Khepera robot that has motorized wheels and a head-mounted video camera (Fig. 1). It is linked to a Linux PC with C/C++ software to numerically process the video stream, integrate it into the motor planning dynamics, and generate motor commands. In this section we describe the perceptual system and the behavioral dynamics of the robot.

A. Perceptual System: Vision

Targets for the robot are defined by their color. The experimenter can interactively set parameters to filter out a particular color (e.g., yellow in Fig. 1) from the video stream. A pixel-array of on/off values is generated for a given HSI-interval of Saturation and Intensity above selected maxima, and of Hue within a selected range. Each pixel location (x, y) is assigned 1 (on) if the pixel-value is within the selected HSI-interval, and 0 (off) if it is not. The hue range is set to encompass the color of the target blocks at different positions and different typical lighting conditions, while the rest of the color spectrum is filtered out. This circumscribes the perceptual cues for the movement targets as on-regions (bottom right in Fig. 1). Two types of input sources are generated from this on/off image: homogeneous boost and task input.

Homogeneous Boost: The homogeneous boost constrains whether to act or not. Activation is boosted everywhere in the field homogeneously whenever the on-pixel count exceeds a given threshold in the left and the right half of the image.

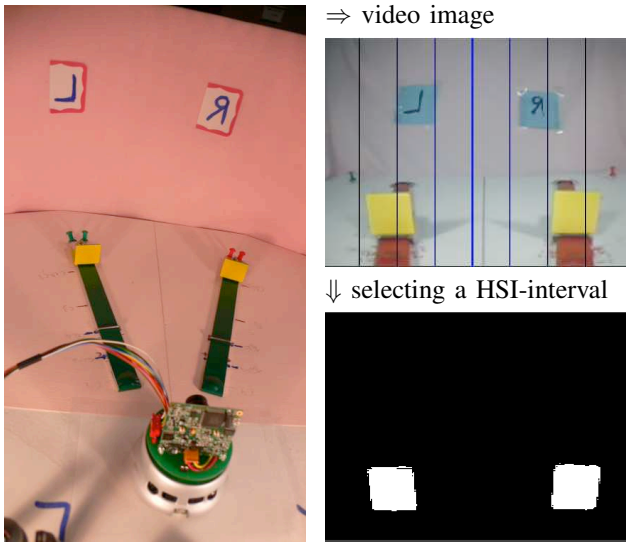

Figure 1. The Khepera robot facing two blocks (left) and the resulting raw (right top) and HSI-filtered (right bottom) images.

It is a non-linear indicator of whether the blocks are within reaching space. If they are far, then the overall tendency to act is low. If they are close, then the activation level in the entire field is boosted, modelling an invitation to act.

Task Input: The task input provides specific location information about targets. For each horizontal viewing direction, the vision system cumulates along the vertical the number of pixels within the selected hue range. Thus, each column provides input with an amplitude that scales with the pixel count so that cues subtending a larger vertical angle provide stronger input (i.e., taller or closer blocks).

The visual input is naturally affected by sensory and environmental noise. To model that perceptual input is in addition subjected to neuronal noise, we apply an Ornstein-Uhlenbeck process $\tau_{\text{noise}}\dot{\eta}_t = -\eta_t + \xi_t$, with $\xi_t \sim N(0,1)$ and a certain latency τ_{noise}. The effect of the neuronal noise scales with the input amplitude. At each horizontal viewing direction ϑ the input value is multiplied with $[1 + A_{\text{noise}}\eta_t(\vartheta)]$, A_{noise} a scalar.

A point spread function—the input profile convolved with a Gaussian bell function—projects the visual input into the motor planning field. For example, input at $\vartheta = -25^\circ$ projects fully to the motor planning neuron encoding -25° and it projects to neighboring neurons with decreasing intensity the further away these neurons are. This models broad receptor tuning curves of the motor planning field.

Coordinate Transformation: When the robot moves, the reference frames of vision (egocentric coordinates) and motor planning (world coordinates) are no longer aligned. To compensate, the transformation from visual to spatial coordinates is based on the dead-reckoned $\tilde{\varphi}$ heading direction of the vehicle. $\tilde{\varphi}$ is realized by path integration, adding up all the small changes $\Delta\varphi$ of the robot's heading direction. The visual map is transposed by $\tilde{\varphi}$ to realign with the spatial motor planning frame.

B. Behavioral Dynamics

Motor Planning Field: The motor planning field $u_{\text{mp}}(\psi)$ is defined over the heading direction ψ of the vehicle. In its core the field is a linear dynamic system with and attractor state at a negative resting level h_{rest}.

$$\tau_{\text{mp}}\dot{u}_{\text{mp}}(\psi) = -u_{\text{mp}}(\psi) + h_{\text{rest}} + \text{boost} + \text{task input} + \text{neural interactions} + \text{preshape}.$$

Perceptual inputs (boost plus task input) and a preshape trace (from motor memory, described below) stimulate the field away from its resting state. If the field becomes positive, then it self-generates activation by means of neural interactions (local excitation and global inhibition). As a whole, the field enters a "working" state whereby it sustains an activation peak. Activated neurons do work—they excite close neighbours and suppress competing inputs elsewhere—to keep the peak stabilized.

The work that the field does for behavior is making and stabilizing decisions. Figure 2a illustrates a sustained peak of activation in the face of two similarly attractive targets (e.g., like in Fig. 1). This peak is maintained despite noise and despite competition from the other target. Without stability, in the face of two identical targets the robot will not be able to approach either: If behavioral was driven directly by the perceptual system, then the fluctuations in the percepts will make the robot wiggle left-right-left-and-so-on, whenever the current precept is strongest. In contrast, as described next, the stable motor planning peaks can govern behavior and generate memory traces of that behavior.

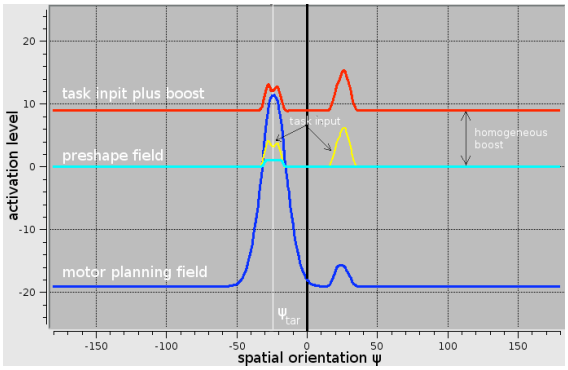

(a) motor planing field, preshape field and inputs

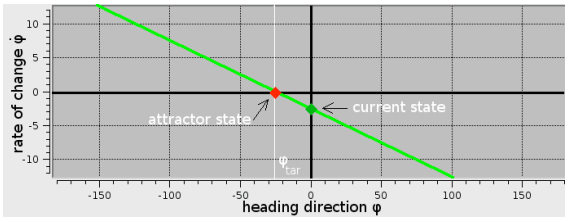

(b) robot's heading direction dynamics

Figure 2. Coupled dynamics of motor planning and turning behavior. Plot (a) shows the level of activation over the spatial orientation ψ in the motor planning field as well as its preshape field and perceptual inputs. Plot (b) shows the heading direction dynamics of the robot. The attractor at φ_{tar} is generated by the motor planning peak at ψ_{tar}.

Motor System: The robot's behavioral dynamics is defined over its heading direction φ and is governed by the motor planning field

$$\tau_{\text{motor}}\dot{\varphi} = -\alpha \int \sigma_{\text{motor}}(u_{\text{mp}}(\psi))(\varphi - \psi)d\psi.$$

The sigmoid σ_{motor} maps positive activation to 1 and negative to 0, α is a scalar that compensates for the width of the peak. In this formalism, attractor states of the motor planning field generate attractors for the robot's heading direction. If the field is entirely below threshold, then the heading direction dynamics is constant at 0, and no movement will be generated. On the other hand, a "working" state of the field with sustained peak activation generates a behavioral attractor. The peak that is centered at ψ_{tar} (Fig. 2a) defines a linear attractor at the corresponding heading direction φ_{tar} (Fig. 2b). The rate of change is translated into revolution signals for the left and right wheels. In fact, at each time step of the numeric integration of the behavioral dynamics, a difference $\Delta\varphi$ is calculated. This difference is then realised by the robot's movement.

Preshape Dynamics: When the robot moves ($\mathcal{X}_{\text{move}} = 1$, else 0), then a motor memory trace is accumulated in the preshape field u_{pre}. It is driven by the motor planning field and it is defined over the same variable ψ

$$\tau_{\text{pre}}\dot{u}_{\text{pre}}(\psi) = \mathcal{X}_{\text{move}} \cdot \left[-u_{\text{pre}}(\psi) + \sigma_{\text{pre}}(u_{\text{mp}}(\psi))\right].$$

The positively activated field sides (mapped to 1 by σ_{pre}, the negative are mapped to 0), leave a local trace in the preshape field (Fig. 2a). Note that the trace comes from the motor planning peak that created the behavioral attractor. This models habit formation: The preshape trace adds activation to the motor planning, thus making it easier to form a motor planning peak at the same location and repeat the action again.

III. *A*-not-*B* Experiment

A. Procedure

The *A*-not-*B* task for the robot is a similar to that for infants. Two blocks (cf. Fig. 1) are moved on tracks back or forward to present a cue and to initiate response. The event sequence of a trial is illustrated in Fig. 3. A trial begins with the robot facing both blocks that are in the distance for 1 second. Next a larger block is placed close to the robot on one side (this is *A*) to cue that location for 4 seconds. The robot is not allowed to move at this moment, but a 3 second delay is imposed. Lastly, both blocks are moved close to the robot, typically providing enough activation to cause an activation peak, making the robot turn to one target. The trial ends with the robot's response, or after 4 seconds if the robot does not respond. At the end of the trial, the field is de-boosted, i.e., activation homogeneously subtracted in the entire field. This destroyed the motor planing peak, allowing for a new trial (in the experiments with infants the toy is taken away to initiate a new trial).

The task has 6 *A* and 2 *B* trials. For training, on the first three trials, the block on the *A* side is somewhat closer to make it more likely for the robot to turn to *A*. Note that this

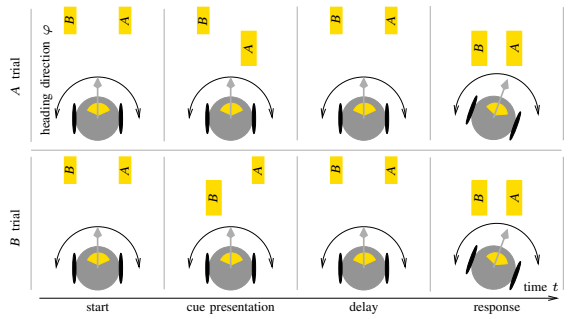

Figure 3. Event sequence on trials of the A-not-B experiment (time axis). The cue is presented at opposite locations on A versus B trials.

procedure is similar to the training done with infants where at the A location the hiding lid is placed closer on the initial trials or a toy is partially visible [11]. Thereafter, both blocks are placed at the same distance from the robot. After six A trials, the B trials are presented. The only difference being that the cue (placing a large block close) is presented at the alternative B location.

The A-not-B task is repeated 12 times. Half the times A is left and B is right, and the other half vice versa. Each task is done with a "naive" robot that has no experience (preshape field is initialized at 0).

B. Analysis

For each experiment we record the robot's response (turn to A, B, or none) per trial; as well as the input stream, motor planning and preshape fields that interact to produce a response. The robot turns correctly to A on 85% of the A trials and makes A-not-B errors on the B trials with 71% of the turns being to A. This replicates the rates of the younger (around 7-month old) infants tested in the A-not-B task [10], [11]. The analysis of the integrated field dynamics explains how the A-not-B errors comes about in the robot.

Figure 4 lays out the field dynamics for trials A_1 and B_1. It shows the typical—correct on A and incorrect on B trials—responses. Showing the large block close induces activation in the motor planning field at the cued location. In both cases, this activation decays during the delay. On the initial A trials, responses are biased to A as the A-site block is placed somewhat closer. When robot turns to A, it accumulates a motor memory trace in the preshape field (cf. Fig. 4a). The trace provides preshape activation to the motor planning field, thus biases further turns to A. In the course of six A trials, the preshape trace grows quite strong as can be seen for trial B_6 in Fig. 4b. This trace biases the robot to turn to A—to make the A-not-B error—on the B trials, although the cue is been then presented at the B location.

Strong evidence for the memory traces comes from the analysis of spontaneous errors [12], which clearly shows that the habit formation in induced by behavior in recently preceding trials. We replicate this finding with the robot, as well a variety of contextual effects, but it exceeds the scope of this paper to discuss them here. Here we focus on testing

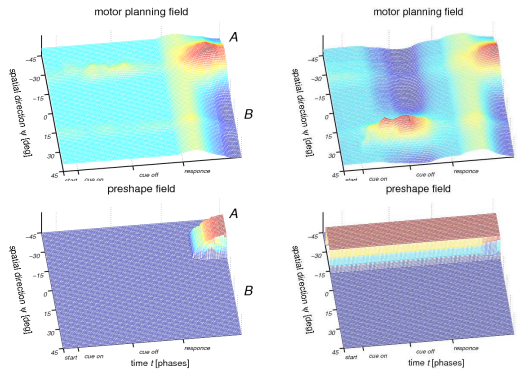

(a) trial A_1 (b) trial B_1

Figure 4. Motor planning (top) and preshape (bottom) on trials A_1 and B_1. The activation level (red: high, blue: low) is plotted for the spatial direction ψ (marks indicate A and B) over time t (marks indicate trial epochs).

the DFT account [4] for infant development in A-not-B.

IV. Age-Delay Effect in A-not-B

The age-delay interaction is the key developmental signature of infant behavior in the A-not-B task [10]. Between 7 and 11 months infants tolerate longer delays before perseverating, while they perseverate gradually less for shorter than the age-typical maximum delay. Critically, infants 12 months and older are correct even after very long delays. The DFT account of A-not-B [4] proposes that neural interactions strengthen over development (modeled as increment of the resting level h_{rest}). Stronger interactions sustain the cue over longer periods of time. We test this developmental account with the robot.

A. Experimental Variations

The resting level for the young robot tested above is $h_{\text{rest}} = -12$. A higher h_{rest} supports the neural interaction in two ways [4], [14]. First, less input is needed to pass the threshold above which the motor planning neurons begin to interact. Then, a higher resting level directly allows for a stronger self-excitation. Figure 5 shows how a field with stronger interactions integrates the specific cue (i.e., placing a block closer).

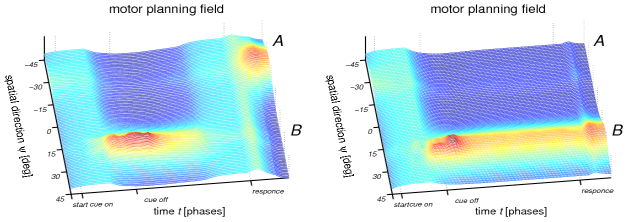

(a) mid-aged robot (b) older robot

Figure 5. Motor planning field on trial B_1 for the mid-aged ($h_{\text{rest}} = -9$, at 7 sec. delay) and older ($h_{\text{rest}} = -7$, at 11 sec. delay) robot.

For the mid-aged robot (Fig. 5a), which has an intermediate level $h_{\text{rest}} = -9$, the cue persists for a longer period then for the youngest robot (Fig. 4b). Thus, despite a strong preshape

trace at A, it is more likely for the robot to follow the cue. The shorter the delay is, the stronger the decision will be guided by the cue.

An even higher resting level brings the dynamics into a different regime where it can self-sustain an activation peak even without additional input [14]. This is the case for the old robot with $h_{\text{rest}} = -7$ (Fig. 5b). Such a peak directs a turn to B after any delay and despite a strong motor trace at A.

B. Statistical Results

We systematically tested the robot in A-not-B task with varying delays and resting levels. For the different resting levels we selected up to three delays, for which we expect performance to vary. Each h_{rest}-delay combination was repeated 12 times. The resulting statistics replicates the age-delay effect, as shown in Figure 6. For instance, a rather young robot ($h_{\text{rest}} = -11$) is correct if there is no delay, it performs around chance for a 2 seconds delay, and it perseverates for a 3 seconds delay. A mid-aged robot ($h_{\text{rest}} = -9$) shows a similar increase of perserveration, but starting at longer delays.

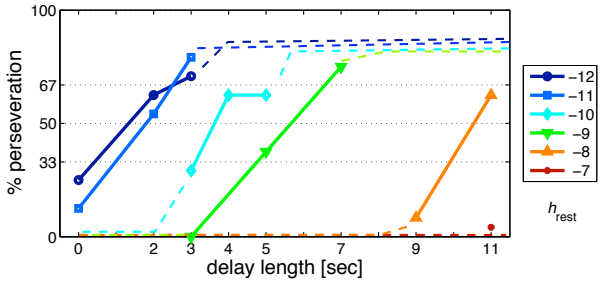

Figure 6. Age-delay interaction for the robot. The rate of perserveration (y-axis) is plotted for different delay lengths (x-axis) and colors code for the different resting levels. The tested delay-h_{rest} combinations are connected by solid lines. The dashed lines (color-coded for the h_{rest}'s) indicate the expected performance for other delays (see text for discussion).

Note that for the mid-aged robot performance is correct at ceiling for the 3 second delay; and shortening the delay will not change this since the cue-induced peak that guides the correct decision is strong also earlier in the delay (Fig. 5a). Similarly, perserveration is at ceiling once the peak has decayed. The dashed lines in Fig. 6 indicate these ceiling effects for the resting levels $h_{\text{rest}} < -7$. The oldest robot with ($h_{\text{rest}} = -7$) is correct for a long delay of 11 seconds. The motor planning peak is persistent (Fig. 5b) and will not decay unless it is actively destructed at the end of a trial (de-boosting). Performance is therefore always correct.

V. Behavioral Demonstration

In this section we investigate the role that motor memory traces might play for stabilizing decisions in a more natural behavioral setting. The robot moves around autonomously in an arena where there are targets and obstacles. Targets, just as in the A-not-B task, are defined by color, may build attractors for the motor planning dynamics to generate behavioral attractors. Obstacles are detected by the robot's infrared (IR) distance sensors and build repellors for the robot's heading direction dynamics (see [15], [16] for a detailed description). This is a simple mechanism to avoid collision.

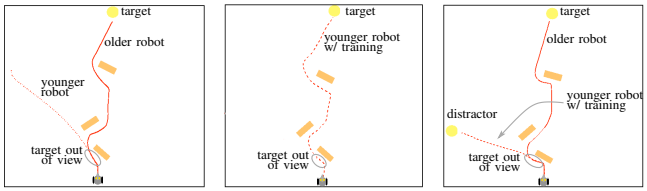

(a) age effect (b) training effect (c) distractor effect

Figure 7. The red lines (young: dotted, young after training: dashed, old: solid) depict the paths when the robot moves autonomously in an arena with targets (yellow cylinders, here circles) avoiding obstacles (wooden blocks, here tan rectangles). The icon shows the robot's initial position and orientation.

Figure 7 shows the basic set-up: from its initial position and orientation, the robot has the distant target in view (cylinders are taller than the blocks). Input from the target builds a peak in the peak motor planning field that builds an attractor for the robot's heading direction dynamics. When the robot begins moving, it avoids the obstacles and loses thereby the target from view. Performance—successful approach of the target—differs for the young and the old robot. Because the young robot's motor planning dynamics is less stable, it can be manipulated by its motor memory or by competitive targets. We illustrate the effects of age, training, and perceptual context in the examples that follow.

A. Age Effect

The performance differences between the young and old robot are shown in Figure 7a. The young robot fails to approach the target. Like in the A-not-B task, it fails to maintain the target location when the target gets out of sight: The motor planning peak decays, and the young robot loses its behavioral attractor. The robot simply stops once it is far enough away from the obstacles. This behavior is comparable to what Piaget's [9] "out of sight, out of mind" stage for young infants who cease to search for an object when it disappears.

The older robot, in contrast, can successfully approach the target despite an obstacle avoidance maneuver. The stronger interactions in its motor planning field are maintaining a peak at the target location even when there is no direct input from the target. This illustrates that one can conceive of the stabilization self-sustained peaks of the motor planning field as a working memory states.

B. Training Effect

Here we illustrate how motor memory may help robust target acquisition. Before tested, the young robot is given some training to simply approach the target without any obstacles in its way. This generates a memory trace in the preshape field for the target direction. The trace stabilizes goal achievement by helping to reestablish a peak representing the target after losing the target from view during an avoidance maneuver. Figure 7b shows the young robot's improved performance—it

successfully approaches the target while avoiding the obstacles. It's trajectory looks very much like that of the older robot in the previous test (Fig. 7a).

This example demonstrates that the accumulation of motor memory in the preshape field is a very simple learning mechanism. The motor memory (which causes the A-not-B error!) supports here working memory by stabilizing the peak that defines the target location. Habit formation is actually a good thing as a process by which previous experience can be utilised for more successful behavior.

C. Distractor Effect

This example illustrates that motor memory does not always help. It is not sufficient to support correct target acquisition when it is brought in conflict with strong perceptual cues. To test this, we place a distractor that looks like the target in the arena, as shown in Figure 7c. The distractor comes into view when the robot turns to avoid the first obstacle. The young robot—despite its preshape trace for the target!—is attracted by the distractor. The young robot displays an "in sight, in mind" behavior. When the distractor comes in view, its input is strong enough to build a new peak in the motor planning field, that destroys the old peak by means of inhibitory interactions. The preshape trace for the target is only local and too weak to prevent the decay of the target peak.

In contrast, the target peak for the old robot is maintained by strong neural interactions. It can therefore successfully approach the target and ignore the competing distractor.

VI. Conclusion

DFT can be embodied. Two fundamental concepts—use of metric dimensions and dynamically stable states—are critical. Substituting the postulated metric input functions of the simulation model with input from the real-time video system only required a few simple filtering operations (here for color, although other features could have been chosen just as well such as visual motion). Because the motor planning field is a dynamical system, and a decision is an attractor state of the system, it is straight forward to couple a behavioral system to the motor planning dynamics: The location of a motor planning peak translates into a behavioral attractor.

With the robotic implementation of the DFT model we achieve quantitative fit of infant perseveration data. We can explain how the A-not-B error comes and goes depending on age and delay with a system that is continously linked to the sensorimotor interface. Importantly, object recognition is not required to account for the data. The system has no hidden and unaccounted for cognitive capacities, such as the object recognition that is required in order for a neuronal unit to represent a visual object [13].

Testing the robot beyond the A-not-B setting suggested a functional interpretation of perseveration as a signature of the habit formation that stabilizes difficult decisions. The memory trace helps to repeat motor actions in a way that makes minimal demands on calibration and alignment of reference frames, a capacity that in itself is far from trivial [17].

Habit formation, however, makes the system inflexible, less able to switch with the cue changes. This reveals a important function of working memory, to stabilize decisions through self-stabilization of the underlying representation of motor goals. This mechanism enhances the flexibility of the system, as it is now capable of following cue changes. This solution makes stronger demands on calibration, because metric working memory requires a stable reference frame which remains invariant between the moment in time at which an instance of working memory is generated and the moment in time at which it is used.

Acknowledgments

The work was funded by NIH grant R37-HD-22830 awarded to Esther Thelen. We thank Esther Thelen, Dexter Gormley, Estela Bicho, and Wolfram Erlhagen.

References

[1] K. Kopecz and G. Schöner, "Saccadic motor planning by integrating visual inforo mation and pre-information on neural, dynamic fields," *Biological Cybernetics*, vol. 73, pp. 49–60, 1995.

[2] C. Wilimzig, S. Schneider, and G. Schöner, "The time course of saccadic decision making: Dynamic field theory," *Neural Networks*, vol. 19, no. 8, pp. 1059–74, 2006.

[3] W. Erlhagen and G. Schöner, "Dynamic field theory of movement preparation," *Psychological Review*, vol. 109, pp. 545–72, 2002.

[4] E. Thelen, G. Schöner, C. Scheier, and L. B. Smith, "The dynamics of embodiment: A field theory of infant perseverative reaching," *Behavioral and Brain Sciences*, vol. 24, no. 1, pp. 1–34, 2001.

[5] A. R. Schutte, J. P. Spencer, and G. Schöner, "Testing the dynamic field theory: Working memory for locations becomes more spatially precise over development," *Child Development*, vol. 74, no. 5, pp. 1393–417, 2003.

[6] S. Perone, J. P. Spencer, and G. Schöner, "A dynamic field theory of visual recognition in infant looking tasks," in *Proceedings from the 29th Annual Meeting of the Cognitive Science Society*, 2007.

[7] J. S. Johnson, J. P. Spencer, and G. Schöner, "Moving to higher ground: The dynamic field theory and the dynamics of visual cognition," *Dynamics and Psychology [special issue]. New Ideas in Psychology*, 2007.

[8] E. Thelen and L. B. Smith, *A Dynamic Systems Approach to the Development of Cognition and Action*. Cambridge, Massachusetts: The MIT Press, A Bradford Book, 1994.

[9] J. Piaget, *The Construction of Reality in the Child*. New York: Basic Books, 1954.

[10] A. Diamond, "Development of the ability to use recall to guide action, as indicated by infants' performance on A-not-B," *Child Development*, vol. 56, pp. 868–38, 1985.

[11] L. B. Smith, E. Thelen, R. Titzer, and D. McLin, "Knowing in the context of acting: The task dynamics of the A-not-B error," *Psychological Review*, vol. 106, no. 2, pp. 235–60, 1999.

[12] E. Dineva, G. Schöner, and E. Thelen, "Behavioral history matters: A dynamic field account of spontaneous and perseverative errors in infant reaching," 2008.

[13] Y. Munakata, "Infant perseveration and implications for object permanence theories: A PDP model of the AB task," *Developmental Science*, vol. 1, no. 2, pp. 161–84, 1998.

[14] S.-I. Amari, "Dynamics of pattern formation in lateral-inhibition type neural fields," *Biological Cybernetics*, vol. 27, pp. 77–87, 1977.

[15] E. Bicho, P. Mallet, and G. Schöner, "Target representation on an autonomous vehicle with low-level representation," *The International Journal of Robotics Research*, vol. 19, pp. 424–47, 2000.

[16] G. Schöner, M. Dose, and C. Engels, "Dynamics of behavior: Theory and applications for autonomous robt architectures," *Robots and Autonomous Systems*, vol. 16, pp. 213–45, 1995.

[17] J. P. Spencer, A. R. Simmering, V R Schutte, and G. Schöner, "What does theoretical neuroscience have to offer the study of behavioral development? Insights from a dynamic field theory of spatial cognition," in *Emerging landscapes of mind: Mapping the nature of change in spatial cognitive development*, J. Plumert and J. P. Spencer, Eds. New York: Oxford University Press, 2007.